

Long-term optical variability of the blazars PKS 2005-489 and PKS 2155-304

T.P. Dominici, Z. Abraham, R. Teixeira and P. Benevides-Soares

*Instituto de Astronomia, Geofísica e Ciências Atmosféricas, Universidade de São Paulo
Rua do Matão 1226, Cidade Universitária, 05508-900, São Paulo, SP, Brazil*

ABSTRACT

We present optical light curves for the period 1996-2000, of two of the brightest known EGRET BL Lac objects: PKS 2005-489 and PKS 2155-304, the latter also one of the few known TeV sources. For both objects, quiescent epochs of low level of variability were followed by active periods, without any indication of periodicity. In PKS 2005-489, several variability events with duration of about 20 days were observed. In PKS 2155-304 fast drops and subsequent rises in luminosity occurred in time scales of days. We proposed an explanation in which a region moving along the relativistic jet is eclipsed by broad line region clouds or star clusters in the host galaxy. We compare our light curves with contemporaneous X-ray observations from All-Sky Monitor/RXTE. Correlations between optical and X-ray activity were not found in any of the sources at long time scales. However in PKS 2005-489 possible correlations were observed in 1997 and 1998 at short time scales, with optical variability preceding X-rays by 30 days in 1997 and succeeding them by about 10 days in 1998. The analysis of the SED, using the optical data presented here and BeppoSAX contemporaneous observations obtained from the literature, shows only small shifts in the synchrotron peak as the X-ray flux density changes.

Subject headings: BL Lacertae objects: general – BL Lacertae objects: individual: PKS 2005-489, PKS 2155-304

1. Introduction

Variability studies are a basic tool to understand the physical processes occurring in AGNs, especially those related to short time scales and high amplitudes, as observed in BL Lacs. In this paper we made use of the five-year database of bright extragalactic sources obtained with the meridian circle of the Abrahão de Moraes Observatory (Valinhos, Brazil), between 1996 and 2000, to study light variations of two EGRET BL Lac sources: PKS 2005-489 and PKS 2155-304.

Both sources are high-frequency peaked BL Lacs (HBLs), with the synchrotron peak located between UV and X-ray wavelengths and were also detected by EGRET in the 100 MeV range (Lin et al. 1999). Moreover, PKS 2155-304 is the only southern hemisphere BL Lac object detected at TeV energies (Chadwick et al. 1999), while PKS 2005-489, also a strong candidate for detection at

this energy range with the available instrumentation (Stecker et al. 1996), has not yet been detected (Chadwick et al. 2000).

The compact nature of PKS 2005-489 at radio frequencies was confirmed by VLBI observations at 5 GHz (Shen et al. 1998). Piner & Edwards (2004) were able to resolve PKS 2155-304 into a core and a jet component at 15 GHz and obtained an upper limit of $4c$ for its apparent velocity. Since even lower velocities were found for the other two TeV blazars observed in that work, the authors concluded that stationary or subluminal velocities seem to be a characteristic of this kind of sources, in contrast with the majority of blazars, for which parsec scale jet components are detected.

The interest in PKS 2005-489 increased after the detection of two strong X-ray flares in 1998 by the Rossi X-Ray Timing Explorer (RXTE, Remillard, 1998, Perlman et al. 1998), however few op-

tical data are available for this object. The only published information about long term variations was presented by Wall et al. (1986), who found a change of 0.5 magnitudes in the B band in two sets of observations spaced by one year. In time scales of a few days, observations in 1994 by Heidt & Wagner (1996) showed 10% amplitude variations in the R band. Similar results were obtained by Rector & Perlman (2003) in observations taken some days after a third X-ray flare in September 2000, while microvariability (variability of minutes to hours) was not detected neither at that epoch nor in 1997 (Romero et al. 1999).

More observations at several wavelengths are available for PKS 2155-304. Using the optical and near infrared data from the literature after 1970, Fan & Lin (2000) suggested the existence of 4 and 7 year periodicity in the light curves. Variability at optical wavelengths in time scales of less than 15 minutes during 1990 was reported by Heidt, Wagner & Wilhein-Erkes (1997) and during 1995 by Paltani et al. (1997). Brightness variations in time scales from few days to minutes were also observed in two large multiband monitoring campaigns, from radio to X-rays, during the last years (e.g. Edelson et al. 1995, Pesce et al. 1997, Urry et al. 1997) and the existence of lags between variability at X-rays and ultraviolet wavelengths verified. However, no microvariability was found by Heidt et al. (1997) in 1994 and by Romero et al. (1999) in 1997 and 1998, showing the existence of a duty cycle for this kind of variability.

In this paper we show that both objects present long time scale variability, alternating between high and low activity. In Section 2 we describe the main aspects of the instrumentation used in this work and the data reduction procedures. The resulting differential light curves are shown in Section 3 and an analysis of the correlation between optical and All-Sky Monitor X-ray data is presented in Section 4. In Section 5 we propose a scenario to explain observed dips in the 1999 light curve of PKS 2155-304. The implication of the data in the spectral energy distribution of the sources is discussed in Section 6. Finally, in Section 7 we summarize our results.

2. Observations and data reduction

The observations were made with the Askania-Zeiss meridian circle, installed at the Abrahão de Moraes Observatory, Valinhos, Brazil ($\phi = 46^\circ 58' 03''$, $\lambda = -23^\circ 00' 06''$). The instrument is a 0.19 m refractor with a focal distance of 2.6 m and has a CCD Thomson 7895A detector (512×512 pixel, with a scale of $1.5''/\text{pixel}$). Observations are made in drift scan mode, where the speed of charge transfer by the CCD is the same as the speed of stellar transit for a fixed instrument position. In this case, the integration time for a declination δ is given by $t_{\text{int}} = 51 \text{ sec } \delta$ seconds (Viateau et al. 1999, Dominici et al. 1999). The observed field has a width of $13'$ in declination and an arbitrary value in right ascension.

The filter used in the instrument is wider than the standard Johnson filter V, with a better coverage for longer wavelengths. The transformation between the magnitudes at the different filters can be estimated from (Dominici et al. 1999):

$$V - V_{\text{Val}} = 0.14 - 0.07(B - V)$$

where V_{Val} designates the magnitudes obtained with the Valinhos system and V and B are the magnitudes in the standard Johnson system.

Our observations started in 1996 and extended to 2000 for PKS 2005-489 and to 1999 for PKS 2155-304. The data are part of an astrometric program directed to the determination of a reference system based on extragalactic sources (Teixeira et al. 1998). Table 1 presents basic information about the observed objects and the observational program. The positions, V magnitudes and redshifts were taken from Véron-Cetty & Véron (1998), the mean value of V_{Val} is given for comparison, t_{int} is the integration time in drift scanning mode and N is the number of processed images for each year.

From the original images, fields of approximately $13' \times 13'$ (512×512 pixel) were extracted. Data reduction was made with the IRAF package¹, using the APPHOT task for aperture photometry in the usual mode, with a median model

¹IRAF is distributed by the National Optical Observatories which is operated by the Association of Universities for research in Astronomy, Inc. under co-operative agreement with the National Science Foundation

to discount the sky contribution and an aperture of three to four times the FWHM. The chosen aperture followed the recommendations of Cellone et al. (2000), to avoid the effects in the resulting light curves of the host galaxies, whose contribution can change due to seeing fluctuations.

Since these light curves were constructed in differential mode, the stability in magnitude of the comparison and control stars is an important factor. Our database with a large time coverage allowed us to quantify this stability. The control stars are the set of field stars chosen to construct a stable reference light curve, represented by the mean magnitude. The stability of the comparison star, from which the differential light curve is constructed, was obtained comparing its magnitude to the mean magnitude of the control stars. Table 2 presents information concerning these stars, most of them are from the Tycho II catalog (Høg et al. 2000). In the first column are the names of the stars and in the second and third their coordinates, the astrometric precision is better than 0.05 arcseconds in average. The fourth column gives the Valinhos magnitude and the last column shows the standard deviation weighted with the individual errors, which are not dependent on the real magnitude values and are good quantitative measures of magnitude stability.

The data selected to construct the light curves for variability analysis have a confidence level of more than 2σ , where σ is the dispersion of the control light curve. However, the errors presented in the light curves were obtained directly from the aperture photometry and, in average, are larger than σ . A few data points in the light curve of PKS 2005-489 seem to follow the same pattern as the control light curve, but were not eliminated because they obey the 2σ criteria.

For the photometric nights, the instrumental magnitudes were calibrated, transformed to the Johnson system and then to flux densities, after correcting by interstellar reddening using the values for visual absorption A_V derived by Bersanelli et al. (1992). The calibration was based on Tycho II stars (Høg et al. 2000) present in the observed fields of the blazars, using the standard procedure adopted in Valinhos's meridian circle data analysis, as described in Dominici et al. (1999) and Viateau et al. (1999).

3. The resulting light curves

Figure 1 shows the light curve of PKS 2005-489 covering all the campaigns. Brightness variations were observed at several time scales, ranging from a few days to years. In particular, even though the time coverage was irregular, we could identify in several occasions similar flare-like variations with monthly time scales. Figure 2 shows five possible peaks superposed and arbitrarily shifted in magnitude and time to emphasize their apparent similarity in shape and duration.

The largest variation in the light curve (about one magnitude in 20 days) was observed in 1998, close to the occurrence of the strong X-ray flares. Except for this short time variation, the mean flux density was lower than those measured in the others years. The behavior of the source just before the X-ray flare that started at the beginning of September 2000 (our observations ended in August 30) was characterized by an increase in optical brightness, also observed with better time resolution by Rector & Perlman (2003). Moreover, the mean flux density for that year was 0.5 magnitude brighter than in 1998.

The light curve of PKS 2155-304 between 1996 and 1999 is shown in Figure 3. It covers some time before and after the TeV and X-ray flares of November 1997 (Chadwick et al. 1999). Although our time coverage is limited, there seems to be a dimming from 1996 to 1998, followed by a chaotic behavior in 1999, when very rapid variations were observed. This is not surprising, since PKS 2155-304 is known to be an intraday variable source (Paltani et al. 1997, for example). However, the mean flux density did not show significant changes in the four years of observation. The maximum variation in our observed 1996 light curve was 0.25 magnitudes, in agreement with the 0.35 magnitudes reported by Bertone et al. (2000) as the results of a short duration multiwavelength campaign in May 1996, just before the beginning of our observations.

We must point out the presence of at least two very sharp dips in the light curve of 1999, with duration of about two days, that are shown in detail in Figure 4. Other dips were reported in the literature at several wavelengths in 1994 (Pesce et al. 1997, Urry et al. 1997) and in polarized light in 1994 and 1998 (Urry et al. 1997, Tommasi et

al. 2001).

The mean flux densities at $\nu = 6.5 \times 10^{15}$ Hz, considering all campaigns, were 30.8 and 23.0 mJy for PKS 2005-489 and PKS 2155-304 respectively. These values lie between the maximum and minimum known flux densities for both sources, as collected by Xie et al. (1998). For PKS 2005-489, the mean flux density measured in 1998 coincides with that predicted by the SED modeled by Padovani et al. (2001), using contemporaneous infrared and X-ray data. However, in 1996 our observed flux density was larger than the value predicted by the same authors, based only in X-ray data.

4. Correlation with X-ray light curves

Correlation of our light curves with data at other frequencies could open more possibilities to the interpretation of the detected brightness variations. For that purpose, we compared our optical observations with the daily averaged X-ray data set in the 1.5 - 12 keV range from RXTE² in the All-Sky Monitor project (ASM, Levine et al. 1996). As X-ray observations present large error bars and our time coverage is in general more sparse, we averaged the X-ray data at several time intervals, calculating their mean values weighted by their errors. The re-sampled X-rays were then compared with the optical light curves to search for correlations at different time scales, using the Discrete Correlation Function (DCF), adequate for unevenly sampled time series. Details of the method could be seen in Edelson & Krolik (1988).

In Figures 5 and 6 we show the optical and X-ray data for PKS 2005-489 and PKS 2155-304, respectively, and in Figures 7 and 8 we present the respective DCF functions including all epochs. We can see that there is no significant correlation between the light curves at time scale of years, independent of the chosen time bins.

We then investigated correlations in time scales of several days in the years for which a reasonable number of optical data points were available. The DCF functions of PKS 2005-489 for 1997, 1998 and 2000 are presented in Figure 9. In 1997 a significant correlation was obtained, with optical emission preceding X-rays; the time lag was about 30 days but the width of the DCF function

did not give a good time resolution. In 1998, on the other hand, the X-rays preceded the optical variability by approximately ten days and no significant correlation was found between the light curves in 2000. Although looking at the optical and X-ray light curves for the individual years one could believe that the significance in the correlations is due to a few high intensity points, this does not seem to be the case, as verified in the DCF function, which remained almost unchanged when those particular data points were excluded from the calculation.

In the case of PKS 2155-304, only for 1999 there were sufficient optical data points to carry out the correlation analysis, which is presented in Figure 10. The results indicate a significant correlation but it is not possible to determine an eventual delay due to the width of the DCF function.

Assuming that the X-rays are produced by the synchrotron process, variations preceding the optical counterpart can be explained by several models, as time-dependent inhomogeneous accelerating jets (Georganopoulos & Marscher 1998) or shocks propagating along the jets (Blandford & Königl 1979, Marscher 1987). The same models can explain the situation in which the optical counterpart appears first, if most of the X-rays were produced by the inverse Compton process, involving synchrotron radio or infrared photons.

5. Dips in the light curve of PKS 2155-304

As mentioned in section 3, we observed several dips in the 1999 light curve of PKS 2155-304, and others were reported previously in the literature. Although a fast decrease in emission can be explained by rapid energy loss from the relativistic electrons, its fast subsequent rise to the previous flux density level is more difficult to understand. For this reason we investigated if eclipses can be the cause of the observed dips. If the eclipsing source is a broad line region cloud, with size 10^{16} cm and velocity of 3000 km s^{-1} , entering the line of sight to the blazar, the time scale for occultation will be of the order of a year, too large to explain our light curve. On the other hand, if it is the eclipsed region that is moving, as in the case of a shock wave propagation along the relativistic jet, with apparent velocity of the order of c , the transit time behind the cloud will be of the order

²<http://xte.mit.edu>

of a few days, as observed. Recent VLBI observations (Piner & Edwards, 2004) showed that a new superluminal feature was formed in 1999, which could be our eclipsed source.

The differences in the dip strength at different wavelengths (Pesce et al. 1997, Urry et al. 1997) could be explained if the eclipsed region and the quiescent jet have different spectral indices. This scenario explains also the polarization effects observed by Urry et al. (1997) and Tommasi et al. (2001). As it is well known from radio observations with high spatial resolution, the polarization properties of the synchrotron radiation in AGNs vary along the jet, especially across the shocks, where the direction and intensity of the magnetic field change drastically. Low resolution observations provide only the average value of the Stokes parameters, and therefore, when one part of the emitting region is eclipsed, the observed average will change with the same time scale.

6. Implications for the SED

The spectral energy distribution (SED) in BL Lacs is usually attributed to emission from a beamed relativistic jet, oriented in a direction very close to the line of sight (Urry & Padovani 1995). The shape of the SED, in the $\log \nu F_\nu \times \log \nu$ representation, usually shows two broad components: the first, with the peak at lower energies, is interpreted as synchrotron emission and the second as inverse Compton by either the photons originated in the synchrotron process (Synchrotron Self Compton, SSC) or by external photons (External Compton, EC). The main problem to model the SED is the lack of simultaneous (or at least contemporaneous) flux density measurements in a large range of energies.

Fortunately, the two studied BL Lacs were observed in contemporaneous epochs by BeppoSAX (Boella et al. 1997), allowing us to construct their spectral energy distribution. PKS 2005-489 was observed in September 1996 and September-December 1998 (Padovani et al. 2001, Tagliaferri et al. 2001) and PKS 2155-304 in November 1996, 1997 and 1999 (Giommi et al. 1998, Chiappetti et al. 1999, Zhang et al. 1999).

Instead of using directly the SED to analyze variability, we started with the flux density distribution, as presented in Figures 11a and 12a

for PKS 2005-489 and PKS 2155-304, respectively. Although the observations are only contemporaneous, it seems that the relative amplitude of the optical variability, if any, is much smaller than that of X-rays. We found that in all cases a smooth curve can describe the flux density distributions, implying a gradual variation of the spectral index from radio to X-rays. For that reason, a parabolic fit was made for each epoch in the $\log F_\nu \times \log \nu$ plane. This procedure has the advantage of being independent of assumptions about the electron energy distribution, which is generally modeled with constant spectral indices and breaks at arbitrary electron energies.

No contemporaneous radio and infrared observations were available, but data from NED (NASA Extragalactic Database) were collected. For PKS 2005-489 we used the infrared data to constrain the fitting while for PKS 2155-304 we used only our optical and BeppoSax data. The fittings can be seen as continuous lines in Figures 11a and 12a for PKS 2005-489 and PKS 2155-304 respectively.

Using this simple flux density distribution we calculated the SED, presented in Figures 11b and 12b for PKS 2005-489 and PKS 2155-304 respectively. The parameters of the fitting in the $\log F_\nu \times \log \nu$ plane, together with the frequency of the maximum (ν_{max}) in the SED, are presented in Table 3. For PKS 2155-304, although no infrared data were used in the fit, the obtained SED coincided with the NED IR data at the epoch of quiescent X-ray emission, as can be seen in Figure 12c. As we can see from Figures 11b and 12b, the radio data lie above the extrapolated SED for both objects, implying that either the flux density distribution is harder at low frequencies, or that part of the radio emission arises from shocks. Notice that although most of the radio data obtained in the literature are from single dish observations and therefore could include extended emission, the observed flat spectrum is an indication that most of the radio emission originates in the compact core.

We can see that for PKS 2005-489, the synchrotron peak frequency in the SED was a factor of four higher in 1998, when the X-ray flare occurred. For PKS 2155-304 the peak frequency was a factor of three higher in 1997, epoch of the detected TeV emission and X-ray counterpart (Chadwick et al. 1999), but it had its minimum value in 1999, epoch of maximum variability in our optical light

curve.

7. Conclusions

This is the first time that a long term optical light curve for PKS 2005-489 is presented. Moreover, the addition of more optical data to the well studied (and yet poorly understood) BL Lac PKS 2155-304 allowed us to confirm that the two studied objects show high degree of variability at different time scales.

In PKS 2005-489 we could identify several variability events with duration of about 20 days, although light curves with better time sampling are necessary to verify if in fact they are arising from similar phenomena. PKS 2155-304 showed a significant activity in short time scales during 1999, with amplitude variations of almost 1 magnitude in a few days. Of special interest is the presence of at least two sharp dips in the light curve, with duration of about two days each. We interpreted them as the result of eclipses, caused by BLR clouds or star clusters in the host galaxy. To obtain the right time scales we had to assume that the the eclipsed region is moving along the jet with relativistic velocities. The detection of a superluminal component formed at that epoch gives support to our assumption (Piner & Edwards 2004). Although our observations cover some months before and after the X and gamma ray activity of 1997, which resulted in the detection of emission at TeV energies (Chadwick et al. 1999), no unusual behavior in the optical light curve was detected at those epochs.

We searched for correlation between the optical light curves and X-rays in the 1.5 - 12 keV range from the All-Sky Monitor project. We did not find significant correlation for any of the sources in time scales of years. However, in time scales of days, we found in PKS 2005-489 possible correlations in the campaigns of 1997 and 1998. In the first year the optical variability preceded the X-rays by approximately 30 days and in 1998 X-rays preceded the optical variability by about 10 days. Although we believe that the optical emission is always due to the synchrotron process, the X-ray activity can be explained also as synchrotron radiation by several models (Georganopoulos & Marscher 1998, Blandford & Königl 1979, Marscher 1987) only when

it precedes the optical variability. Otherwise the same models can be applied, but assuming the the X-ray emission is due to the inverse Compton process involving synchrotron radio or infrared photons. The 1999 optical and X-ray light curves of PKS 2155-304 seems to be correlated, but it was not possible to determine the presence of time delays because of the width of the DCF function.

We also constructed the SED with our optical data and contemporaneous BeppoSAX X-ray observations. First we fitted a simple parabola in the $\log F_\nu \times \log \nu$ plane and then constructed the SED, instead of using multi-parametric models, as usually done (eg. Padovani et al. 2001). Although the observation are only contemporaneous, it seems that the relative amplitude of the optical variability, if any, is much smaller than that of X-rays. The obtained SEDs confirm that the synchrotron peaks move to higher frequencies during the occurrence of X-ray flares, although the shifts were much smaller than what was observed for other blazars (Pian et al. 1998, Giommi et al. 1999).

This work was partially supported by the Brazilian agencies FAPESP, CNPq and FINEP. We thank the referee for the comments that helped us to improve significantly this paper and A. Caproni for interesting discussions. This research made use of the NASA/IPAC Extragalactic Database (NED), which is operated by the Jet Propulsion Laboratory, California Institute of Technology, under contract with the National Aeronautics and Space Administration.

REFERENCES

Bersanelli, M., Bouchet, P., Falomo, R. & Tanzi, E.G., 1992, AJ, 104, 28

Bertone, E., Tagliaferri, G., Ghisellini, G., Treves, A., Barr, P., Celotti, A., Chiaberge, M. & Maraschi, L. 2000, ApJ, 356, 5

Blandford, R. & Königl, A., 1979, ApJ, 232, 34

Boella, G., Butler, R.C., Perola, G.C., Piro, L., Scarsi, L. & Bleeker, J.A.M., 1997, A&AS, 122, 299

Cellone, S.A., Romero, G.E. & Combi, J.A., 2000, AJ, 119, 1534

Chadwick, P.M., Lyons, K., McComb, T.J.L., Orford, K.J., Rayner, S.M., Shaw, S.E., Turver, K.E., & Wieczorek, G.J., 1999 *ApJ*, 513, 161

Chadwick, P.M., Daniel, M.K., Lyons, K., McComb, T.J.L., McKenny, J.M., Nolan, S.J., Orford, K.J., Osborne, J.L., Rayner, S.M. & Turver, K.E., 2000, *A&A*, 364, 450

Chiappetti, L., Maraschi, L., Tavecchio, F., Celotti, A., Fossati, G., Ghisellini, G., Giommi, P., Pian, E., Tagliaferri, G., Treves, A., Urry, C.M. & Zhang, Y.H., 1999, *ApJ*, 521, 552

Dominici, T.P., Teixeira, R., Horvath, J.E., Medina Tanco, G.A. & Benevides-Soares P., 1999, *A&AS*, 136, 261

Edelson, R., Krolik, J., Madjeski, G. et al., 1995, *ApJ*, 438, 120

Edelson, R.A. & Krolik, J.H., 1988, *ApJ*, 333, 646

Falomo, R., Pesce, J.E. & Treves, A., 1993, *ApJ*, 411, L63

Fan, J.H. & Lin, R.G., 2000, *A&A*, 355, 880

Georganopoulos M. & Marscher A.P., 1998, *ApJ*, 506, L11

Ghisellini, G., Maraschi, L. & Treves, A., 1985, *A&A*, 146, 204

Giommi, P., Fiore, F., Guainazzi, M. et al, 1998, *A&A*, 333, L5

Heidt, J. & Wagner, S.J., 1996, *A&A*, 305, 42

Heidt, J., Wagner, S.J. & Wilhein-Erkes, U., 1997, *A&A*, 325, 27

Høg, E., Fabricius, C., Makarov, V.V., Urban, S., Corbin, T., Wycoff, G., Bastian, U., Schwekendiek, P. & Wicenec, A., *A&A*, 357, 367, 2000

Levine, A.M., Bradt, H., Cui, W. et al., 1996, *ApJ*, 469, L33

Lin, Y.C., Bloom, S.D., Esposito, J.A., Hartman, R.C., Hunter, S.D., Kanbach, G., Kniffen, D.A., 1999, *ApJ*, 525, 191

Marscher A.P., in "Superluminal Radio Sources", eds. Zensus J.A. & Pearson T.J., Cambridge University Press, 280, 1987

Padovani, P., Costamante, L., Giommi, P., Ghisellini, G., Comastri, A., Wolter, A., Maraschi, L., Tagliaferri, G. & Urry, C., 2001, *MNRAS*, 328, 931P

Paltani, S., Courvoisier, T.J.-L., Blecha, A. & Bratschi, P., 1997, *A&A*, 327, 539

Perlman, E.S., Madejski, G., Stocke, J. T. & Rector, T.A., 1999, *ApJ*, 523, L11

Pesce, J.E., Urry, C.M., Maraschi, L. et al., 1997, *ApJ*, 486, 770

Piner, B.G. & Edwards, P.G., *ApJ*, 600, 115, 2004

Rector, T.A., & Perlman, E.S., 2003, *AJ*, 126, 47

Remillard, R., 1998, *IAUC* 7041

Romero, G.E, Cellone, S.A. & Combi, J.A., 1999, *A&AS*, 135, 477

Sambruna, R.M., Urry, C.M., Ghisellini, G. & Maraschi, L., 1995, *ApJ*, 449, 567

Shen, Z.-Q., Wan, T.-S., Moran, J.M. et al., 1998, *AJ*, 115, 1357

Stecker, F.W., de Jager, O.C. & Salamon, M.H., 1996, *ApJL*, 473, 75.

Tagliaferri, G., Ghisellini, G., Giommi, P., Celotti, A., Chiaberge, M., Chiappetti, L., Glass, I.S., Maraschi, L., Tavecchio, F., Treves, A. & Wolter, A., 2001, *A&A*, 368, 38

Teixeira, R., Benevides-Soares, P., Dominici, T.P., Monteiro, W., Rapaport, M., LeCampion, J.F & Réquiéme, Y., 1998, *AcHA*, 3, 190

Tommasi, L., Diaz, R., Palazzi, E., Pian, E., Poretti, E., Scaltrini, F. & Treves, A., 2001, *ApJL*, 132, 73.

Urry, M.C. & Padovani, P., 1995, *PASP*, 107, 803

Urry, M.C., Treves, A., Maraschi, L. et al., 1997, *ApJ*, 486, 799

Véron-Cetty, M.P & Véron, P., 1998, "A catalogue of Quasars and Active Galactic Nuclei" (8o edition), ESO Scientific Report, 18

Viateau, B., Réquie, Y., Le Campion, J.F.,
Benevides-Soares, P., Teixeira, R., Montignac,
G., Mazurier, J.M., Monteiro, W., Bosq, F.
Chauvet, F., Colin, J., Daigne, G., Desbats,
J.M., Dominici, T.P., Périé, J.P., Rafaelli, J.
& Rapaport, M., 1999, A&AS, 134, 173

Xie, G.Z., Zhang, X., Bai, J.M. & Xie, Z.H., 1998,
ApJ, 508, 180

Zhang, Y.H., Cellotti, A., Treves, A., et al., 1999,
ApJ, 527, 719

Wall, J.V., Danziger, M., Pettini, M., Warwick,
R.S. & Wamsteker, W., 1986, MNRAS, 219,
23P

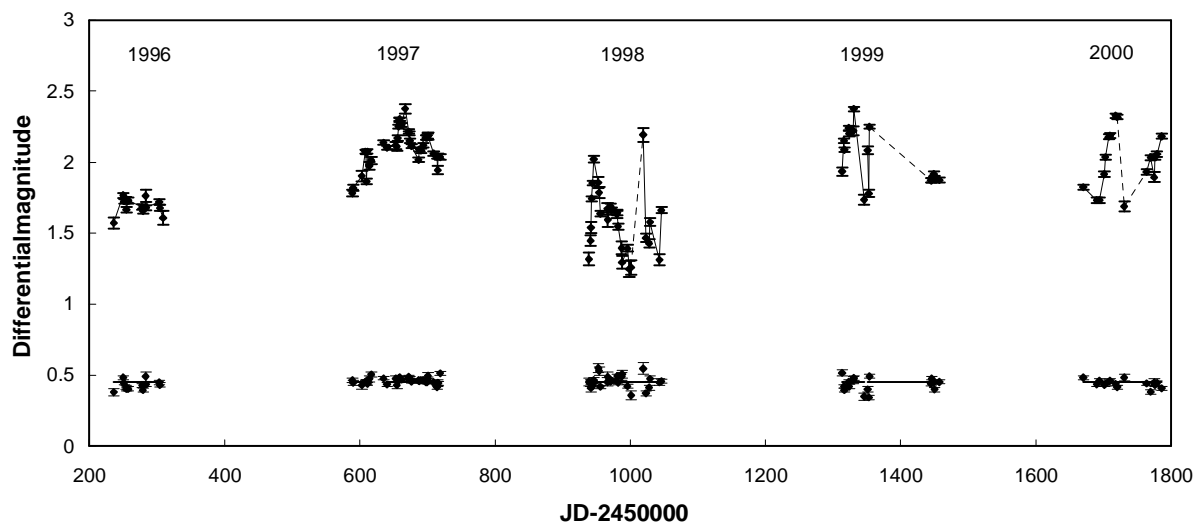


Fig. 1.— Differential light curve of the BL Lac PKS 2005-489 from 1996 to 2000: upper curve, C2-O, where O is the source. The control light curve is shown below and was constructed with C2 minus the mean among C1, C3 and C4 (see Table 2). The dashed lines indicate time intervals of more than ten days without observations.

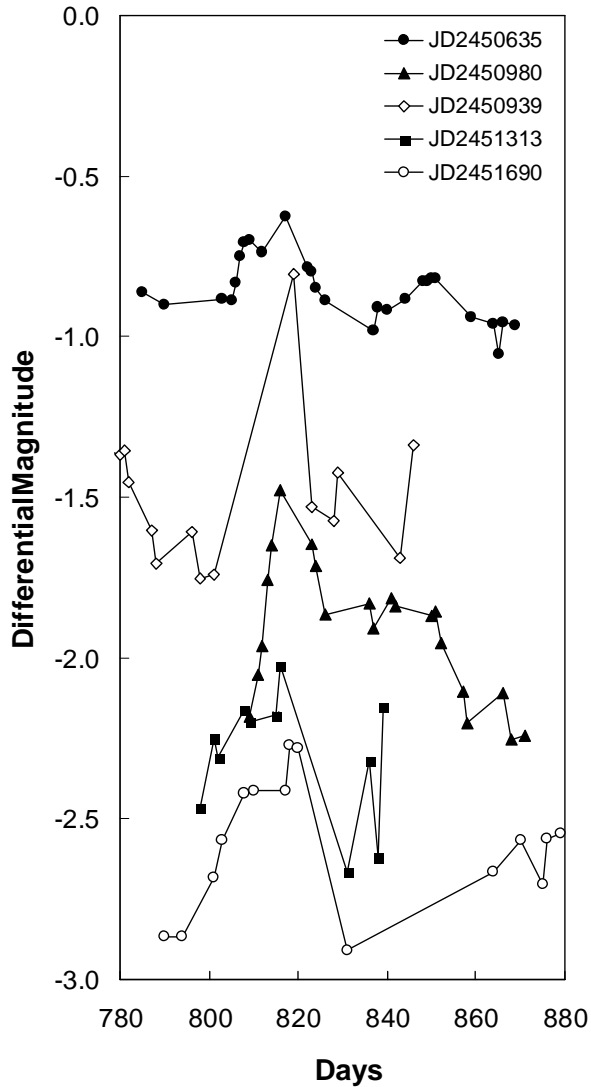


Fig. 2.— Superposition of the peaks detected in 1997, 1998, 1999 and 2000 light curves of the BL Lac PKS 2005-489. The magnitude scale was arbitrary shifted for better comparison. The legend inside the figure indicated the epoch of the first point in each curve.

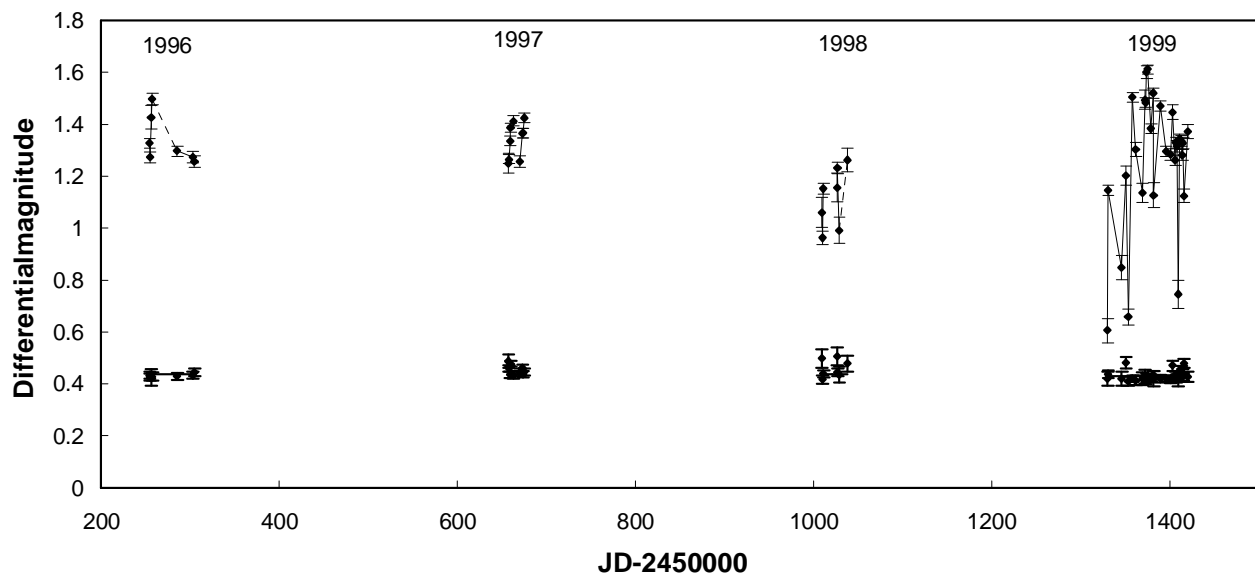


Fig. 3.— Differential light curve of the BL Lac PKS 2155-304 from 1996 to 2000. Upper curve: C2-O, where O is the source. The control light curve is shown below and was constructed with C2 minus the mean between C1 and C3 (see Table 2). The dashed lines are as in Figure 1.

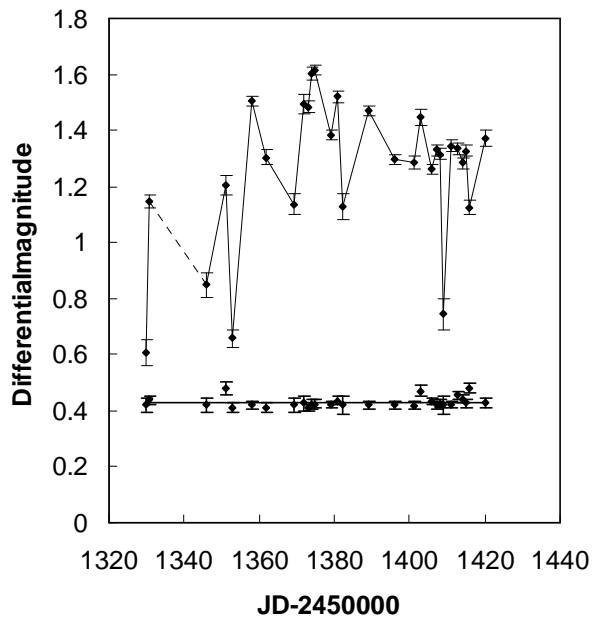


Fig. 4.— Upper curve: differential light curve of the BL Lac PKS 2155-304 in 1999. Lower curve: the control light curve. The dashed lines are as in Figure 1.

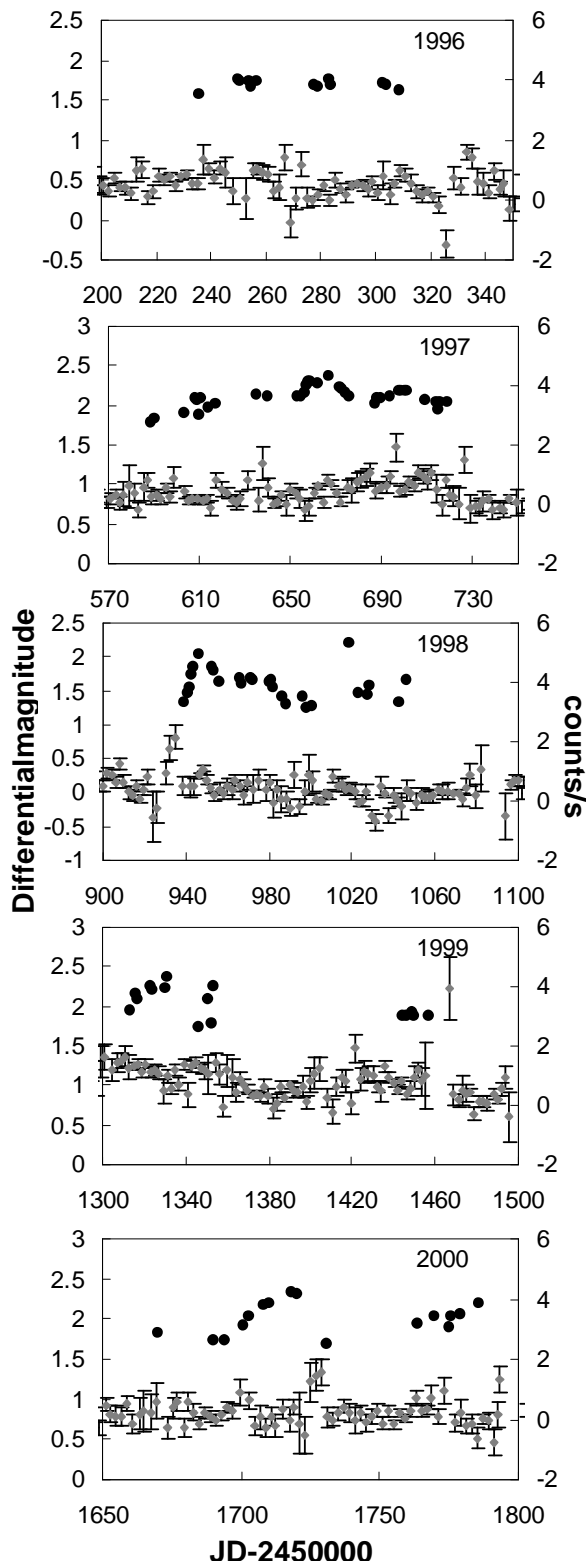


Fig. 5.— Comparison between the optical light curves (black points) of PKS 2005-489 and the contemporaneous X-rays ASM data in the 1.5 - 12 KeV range, from 1996 to 2000. In this example, the X-rays data were binned by calculating the weighted mean value of two points separated by no more than 4 days

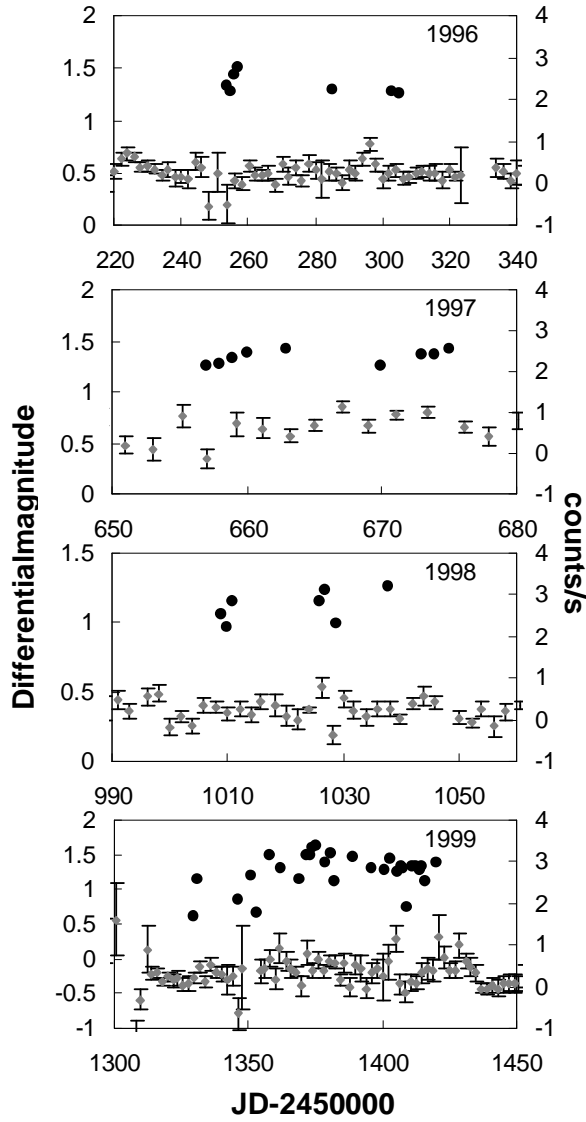


Fig. 6.— Comparison between the optical light curves (black points) of PKS 2155-304 and the contemporaneous X-rays ASM data in the 1.5 - 12 KeV range, from 1996 to 1999. In this example, the X-rays data were binned by calculating the weighted mean value of two points separated by no more than 4 days

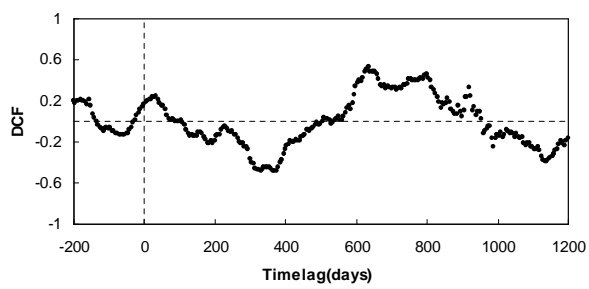


Fig. 7.— Discrete correlation function (DCF) between optical and X-ray data for PKS 2005-489 using the complete dataset and a bin size of 40 days.

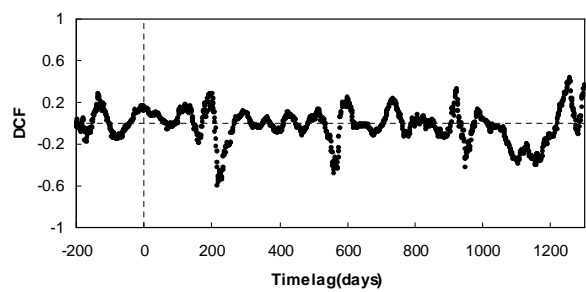


Fig. 8.— Discrete correlation function (DCF) between optical and X-ray data for PKS 2155-304 using the complete dataset and a bin size of 40 days.

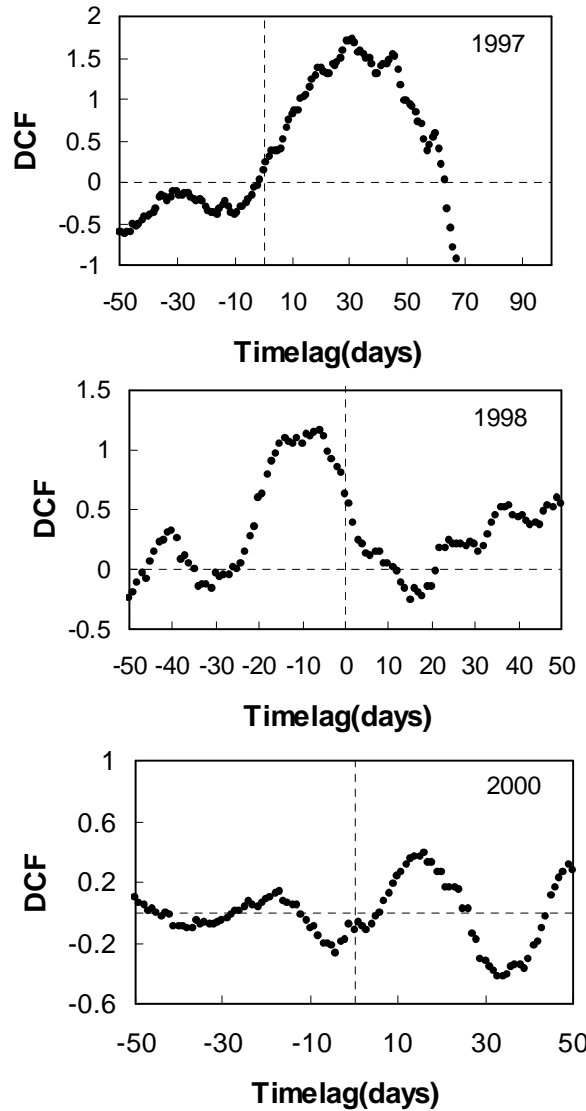


Fig. 9.— Discrete correlation function for PKS 2005-489 in 1997, 1998 and 2000. In all cases the bin size was 20 days.

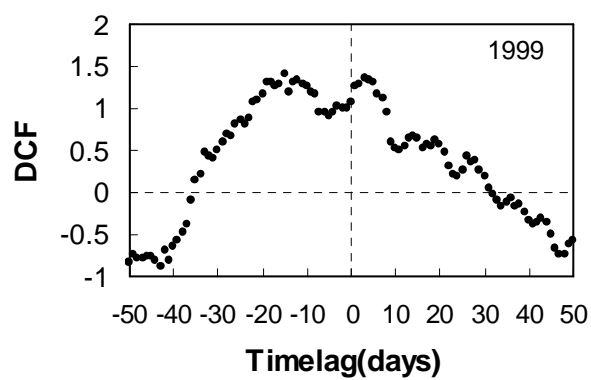


Fig. 10.— Discrete correlation function for PKS 2155-304 in 1999. The bin size was 20 days.

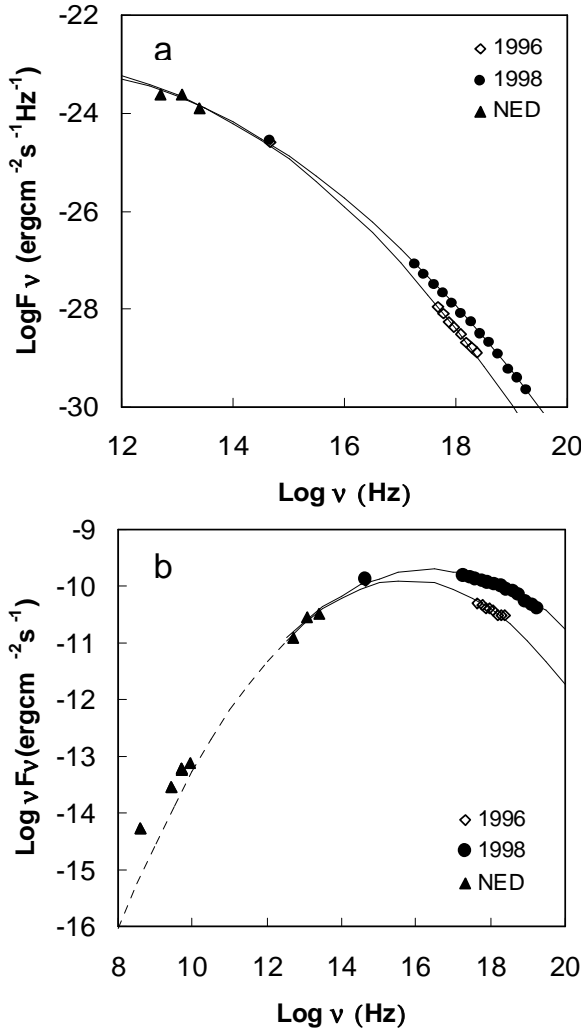


Fig. 11.— Spectral energy distribution of PKS 2005-489 in 1996 and 1998, using two different representations: a) $\log F_\nu \times \log \nu$ and b) $\log \nu F_\nu \times \log \nu$. The X-ray data are BeppoSAX observations presented by Padovani et al. (2001). The data from infrared and radio wavelengths were obtained in NED Database. The lines indicate parabolic fits from infrared to X-ray data in the $\log F_\nu \times \log \nu$ plane (see text for details).

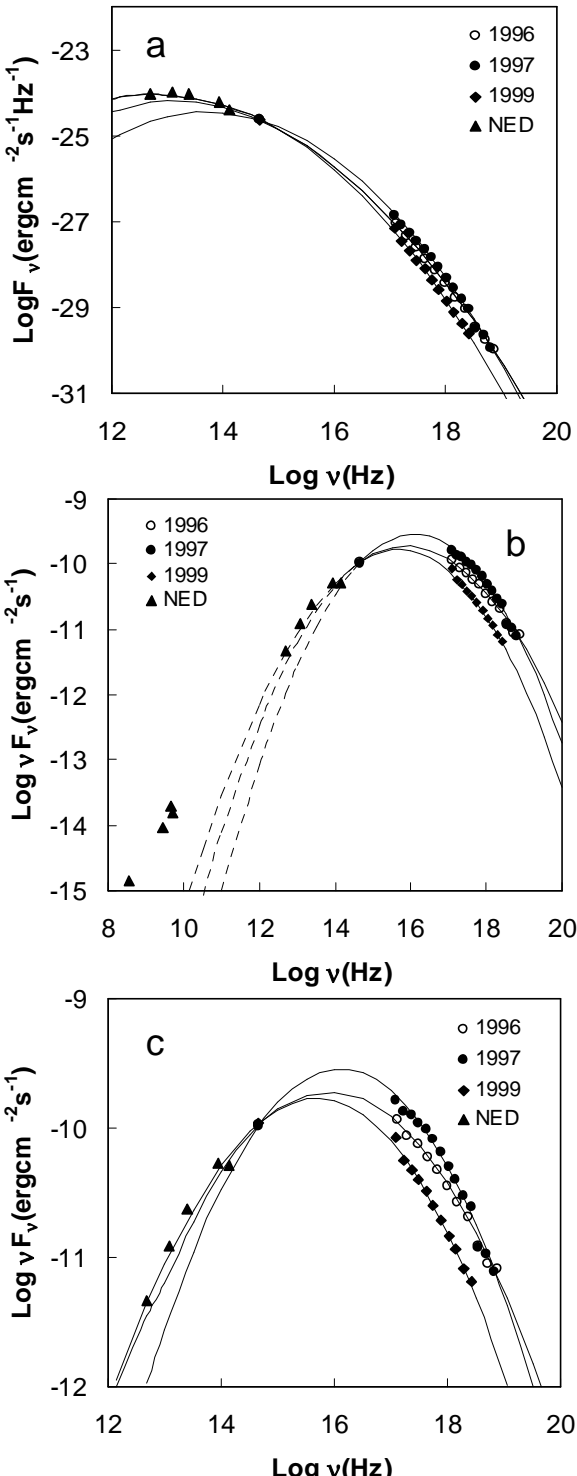


Fig. 12.— Spectral energy distribution of PKS 2155-304 in 1996, 1997 and 1999, using two different representations: a) $\log F_\nu \times \log \nu$ and b) $\log \nu F_\nu \times \log \nu$. c) same as b) in an expanded frequency scale. The X-ray data are BeppoSAX observations presented by Giommi et al. (1998), Chiappetti et al. (1999) and Zhang et al. (2002). The data from infrared and radio wavelengths were obtained in NED Database and are not contemporaneous. The lines indicate parabolic fits to the

TABLE 1
BASIC DATA OF THE OBSERVED SOURCES AND THE OBSERVATIONAL PROGRAM.

Object	α (J2000)	δ (J2000)	V	V _{val}	z	t_{int} (s)	Date	N
PKS 2005-489	20 09 25.39	-48 49 53.7	13.4	13.0	0.071	78.5	05/31 - 08/13/1996	13
							05/19 - 09/27/1997	37
							05/05 - 08/20/1998	27
							05/14 - 10/06/1999	16
							05/05 - 08/30/2000	16
PKS 2155-304	21 58 52.06	-30 13 32.1	13.1	13.1	0.170	59.8	06/18 - 08/08/1996	7
							05/31 - 08/13/1997	9
							07/14 - 08/12/1998	7
							05/31 - 08/30/1999	29

TABLE 2

STARS CHOSEN FOR REFERENCE AND CONTROL IN THE FIELD OF THE STUDIED OBJECTS.

Object	α (J2000)	δ (J2000)	V_{val}	sigma
PKS 2005-489				
C1 (8400 1817)	20 09 23.25	-48 52 30.2	9.25	0.0003
C2 (8400 900)	20 09 05.42	-48 47 20.9	11.88	0.0018
C3 (8400 620)	20 09 48.72	-48 48 51.6	12.20	0.0018
PKS 2155-304				
C1 (7488 124)	21 59 01.52	-30 09 29.9	9.18	0.0033
C2 (7488 340)	21 59 02.51	-30 10 46.6	12.14	0.0044
C3	21 59 05.33	-30 10 51.1	12.96	0.0069
C4	21 58 46.51	-30 17 51.3	12.76	0.0062

TABLE 3

PARAMETERS OF THE PARABOLIC FITS AND FREQUENCY OF THE SYNCHROTRON PEAK FOR EACH EPOCH

Object	Epoch	quadratic	linear	constant	χ^2/dof	ν_{peak} (Hz)
PKS 2005-489	1996	-0.10	2.521	-35.19	0.04/10	5.6×10^{15}
	1998	-0.08	1.58	-30.89	0.02/15	2.5×10^{16}
PKS 2155-304	1996	-0.16	4.07	-50.00	0.02/9	7.9×10^{15}
	1997	-0.21	5.76	-63.93	0.03/15	1.3×10^{16}
	1999	-0.20	5.18	-58.26	11.31/9	5.0×10^{15}